Journal of the American College of Cardiology
© 2010 by the American College of Cardiology Foundation
Published by Elsevier Inc.

Vol. 56, No. 10, 2010
ISSN 0735-1097/$36.00
doi:10.1016/j.jacc.2010.03.070

QUARTERLY FOCUS ISSUE: HEART RHYTHM DISORDERS

Calcium Dynamics and the Mechanisms of Atrioventricular Junctional Rhythm

Daehyeok Kim, MD, PHD,* Tetsuji Shinohara, MD, PHD,* Boyoung Joung, MD, PHD,* Mitsunori Maruyama, MD, PHD,* Eue-Keun Choi, MD, PHD,* Young Keun On, MD, PHD,* Seongwook Han, MD, PHD,* Michael C. Fishbein, MD,† Shien-Fong Lin, PHD,* Peng-Sheng Chen, MD*

Indianapolis, Indiana; and Los Angeles, California

Objectives The purpose of this study was to test the hypothesis that rhythmic spontaneous sarcoplasmic reticulum calcium (Ca) release (the "Ca clock") plays an important role in atrioventricular junction (AVJ) automaticity.

Background The AVJ is a primary backup pacemaker to the sinoatrial node. The mechanisms of acceleration of AVJ intrinsic rate during sympathetic stimulation are unclear.

Methods We simultaneously mapped transmembrane potential and intracellular Ca in Langendorff-perfused canine AVJ preparations that did not contain sinoatrial node (n = 10).

Results Baseline AVJ rate was 37.5 ± 4.0 beats/min. The wavefront from leading pacemaker site propagated first through the slow pathway, then the fast pathway and atria. There was no late diastolic Ca elevation (LDCAE) at baseline. Isoproterenol up to 3 μmol/l increased heart rate to 100 ± 6.8 beats/min, concomitant with the appearance of LDCAE that preceded the phase 0 of action potential by 97.3 ± 35.2 ms and preceded the onset of late diastolic depolarization by 23.5 ± 3.5 ms. Caffeine also produced LDCAE and AVJ acceleration. The maximal slope of LDCAE and diastolic depolarization always colocalized with the leading pacemaker sites. Ryanodine markedly slowed the rate of spontaneous AVJ rhythm. Isoproterenol did not induce LDCAE in the presence of ryanodine. The I_f blocker ZD 7288 did not prevent LDCAE or AVJ acceleration induced by isoproterenol (n = 2).

Conclusions Isoproterenol and caffeine induced LDCAE and accelerated intrinsic AVJ rhythm. Consistent colocalization of the maximum LDCAE and the leading pacemaker sites indicates that the Ca clock is important to the intrinsic AVJ rate acceleration during sympathetic stimulation. (J Am Coll Cardiol 2010;56:805–12) © 2010 by the American College of Cardiology Foundation

The mechanisms of automaticity have traditionally been attributed to the actions of multiple time- and voltage-dependent membrane ionic currents. However, recent studies showed that in addition to these membrane ionic clocks, rhythmic spontaneous sarcoplasmic reticulum (SR) Ca release (the "Ca clock") can result in rhythmic sodium-calcium exchange current (I_{NCX}) activation and sinoatrial node (SAN) depolarization (1,2). We recently confirmed that the membrane ionic clock worked synergistically with the Ca clock to generate sinus rhythm in dogs (3). Whether or not Ca clock contributed to heart rhythm generation in other parts of the heart was unclear. Atrioventricular junction (AVJ) contains specialized conduction tissues, including proximal atrioventricular (AV) bundle, His bundle, and AV node (4). These specialized structures may participate in AVJ automaticity (5). The AVJ is also a common source of cardiac arrhythmia. However, relatively little is known about the mechanisms of automaticity in the AVJ. It has been demonstrated that I_{NCX} is present in cells from rabbit atrioventricular node (AVN), and removal of external Na produced a rise of intracellular Ca (Ca_i) through the reverse mode of I_{NCX} (6,7). It is also known that the rate of

From the *Krannert Institute of Cardiology and the Division of Cardiology, Department of Medicine, Indiana University School of Medicine, Indianapolis, Indiana; and the †Department of Pathology and Laboratory Medicine, University of California–Los Angeles, Los Angeles, California. Dr. Kim is currently at the Department of Internal Medicine, Inha University Hospital, Incheon, South Korea. Supported by the National Institutes of Health/National Heart, Lung, and Blood Institute grants P01 HL78931, R01 HL78932, and 71140; a Korean Ministry of Information and Communication through research and develop support project (Dr. Joung); a Nihon Kohden/St. Jude Medical electrophysiology fellowship (Dr. Maruyama); a Korea Research Foundation Grant (KRF-2008-357-E00028) funded by the Korean Government (Dr. Choi); a Piansky Family Endowment (Dr. Fishbein); an American Heart Association Established Investigator Award (Dr. Lin); and a Medtronic-Zipes Endowment (Dr. Chen). Medtronic Inc., St. Jude Medical, and Cryocath Inc. donated research equipment. All other authors report that they have no relationships to disclose.

Manuscript received December 24, 2009; revised manuscript received February 26, 2010, accepted March 30, 2010.

JACC Vol. 56, No. 10, 2010
August 31, 2010:805–12

Abbreviations and Acronyms

AU = arbitrary unit
AV = atrioventricular
AVJ = atrioventricular junction
AVN = atrioventricular node
Ca_i = intracellular calcium
DD = diastolic depolarization
FP = fast pathway
HCN4 = hyperpolarization-activated cyclic nucleotide-gated potassium channel 4
I = membrane ionic current
LDCAE = late diastolic calcium elevation
LP = leading pacemaker
SAN = sinoatrial node
SP = slow pathway
SR = sarcoplasmic reticulum
TZ = transitional zone
V_m = transmembrane potential

spontaneous activity of myocytes isolated from rabbit AVN may be decreased by ryanodine and increased by isoproterenol. These changes are accompanied by a decrease and an increase, respectively, in the slope of the preceding Ca ramp (8). These findings suggest that subcellular Ca_i dynamics (the Ca clock) may contribute to the automaticity of the AVJ. However, this hypothesis has not been tested in intact AVJ preparations. We hypothesize that Ca clock is important in AVJ automaticity in intact canine AVJ preparations and that isoproterenol accelerates AVJ rhythm through the increased magnitude of SR Ca release. The purpose of this study is to perform simultaneous transmembrane potential (V_m) and Ca_i mapping to test these hypotheses in a canine model.

Methods

This study protocol was approved by the Institutional Animal Care and Use Committee of Indiana University. Hearts from 10 normal mongrel dogs were excised under general anesthesia and were perfused through the aorta with cardioplegic solution. The proximal right and left circumflex arteries were separately cannulated (9). The AVJ preparations (Fig. 1A) were perfused with Tyrode's solution at 37°C with 95% O_2 and 5% CO_2 to maintain a pH of 7.4 through the coronary cannula. The composition of Tyrode's solution was NaCl 125 mmol/l, KCl 4.5 mmol/l, NaH_2PO_4 1.8 mmol/l, $NaHCO_3$ 24 mmol/l, $MgCl_2$ 0.5 mmol/l, $CaCl_2$ 1.8 mmol/l, and glucose 5.5 mmol/l. Albumin 100 mg/l was added in deionized water. Contractility was inhibited by 10 to 17 μmol/l of blebbistatin. Pseudo electrocardiogram was recorded with bipolar electrodes in the right atrium. A multipolar electrophysiological catheter was used to record the His bundle electrogram.

Optical mapping. We performed simultaneous dual optical mapping of V_m and Ca_i while the hearts were Langendorff perfused (3). After mapping of baseline spontaneous beats, pharmacologic intervention was performed. All 10 hearts were mapped both at baseline and during pharmacologic intervention. Among them, 4 were used for

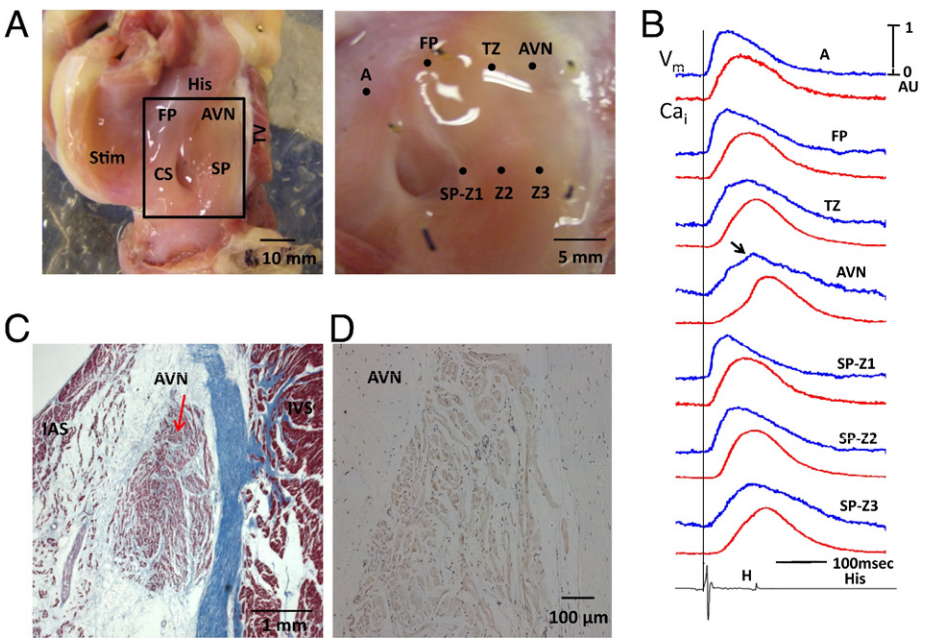

Figure 1 Gross Anatomy and Histology of the AVJ Preparation

(A) Left panel shows the atrioventricular junction (AVJ) preparation used in the study. The **area outlined by the rectangle** was the area mapped. The **right panel** shows the area mapped in greater detail. **(B)** The optical signals from the labeled sites are shown. The **blue line** is the optical transmembrane potential (V_m), whereas the **red line** is optical intracellular calcium (Ca_i) tracing. The **arrow** points to an additional hump on the atrioventricular node (AVN), which corresponded to the His bundle potential **(B, bottom)**. A **vertical line** indicates the beginning of atrial pacing spike. The pacing cycle length was 600 ms. **(C)** Histology of a transmural section through the AVN **(arrow)**. The slide was stained with Masson's trichrome stain (×100). **D** shows positive **(brown)** immunostaining of HCN4 in the AVN but not in the surrounding tissues. CS = coronary sinus; FP = fast pathway; IAS = interatrial septum; IVS = interventricular septum; SP = slow pathway; SP-Z1, 2, and 3 = slow pathway zones 1, 2, and 3, respectively; TV = tricuspid valve; TZ = transitional zone.

β-adrenergic stimulation with isoproterenol. In 2 hearts, ryanodine (3 μmol/l) was used without and with isoproterenol (1 μmol/l) infusion. In the remaining 4 hearts, we performed the following pharmacologic interventions: caffeine infusion (20 mmol/l given as a bolus in 1 s, n = 2), ZD 7288 (3 μmol/l), followed by isoproterenol (1 μmol/l, n = 2).

Histology. The tissues were fixed in formalin, and the AVJ region was sectioned into 5 rectangular blocks as described by Inoue and Becker (10). The tissues were paraffin embedded, sectioned, and stained with hematoxylin and eosin and with Masson's trichrome stain. In addition, we performed immunostaining of hyperpolarization-activated cyclic nucleotide-gated potassium channel 4 (HCN4) with rabbit anti-HCN4 polyclonal antibody (Santa Cruz Biotechnology Inc, Santa Cruz, California).

Data analysis. The Ca_i and V_m traces were normalized to their respective peak-to-peak amplitude for comparison of timing and morphology. We assign the maximum amplitude of Ca_i and V_m during baseline pacing as 1 arbitrary unit (AU). The amplitude and the slope of the late diastolic Ca elevation (LDCAE) were expressed as AU and AU/s, respectively (3). The same applies to diastolic depolarization (DD) detected on the V_m tracings. To generate an isochronal map, the optical mapping data were spatiotemporally filtered with a 3 × 3 × 3 moving average operation. The activation time at each pixel was determined by threshold crossing, usually set at the mid-point of the optical action potential. The activation isochrones were then constructed by grouping the pixels with the same activation time. Paired *t* tests were used to compare the means at baseline and during pharmacologic intervention in the same preparation. Analysis of variance with Bonferroni post hoc test was used to compare the slopes of LDCAE and DD at different distances and with different doses of isoproterenol. Data were presented as mean ± standard error of the mean. A p value of ≤0.05 was considered statistically significant.

Results

Anatomy of the AVJ. A picture of the AVJ preparation is shown in Figure 1A. The rectangle in the left panel was enlarged and shown at the right. The optical signals during atrial pacing (600-ms cycle length) at different sites are shown in Figure 1B. The locations of the fast pathway (FP), slow pathway (SP), transitional zone (TZ), and AVN were determined both by its anatomical locations (10) and by the

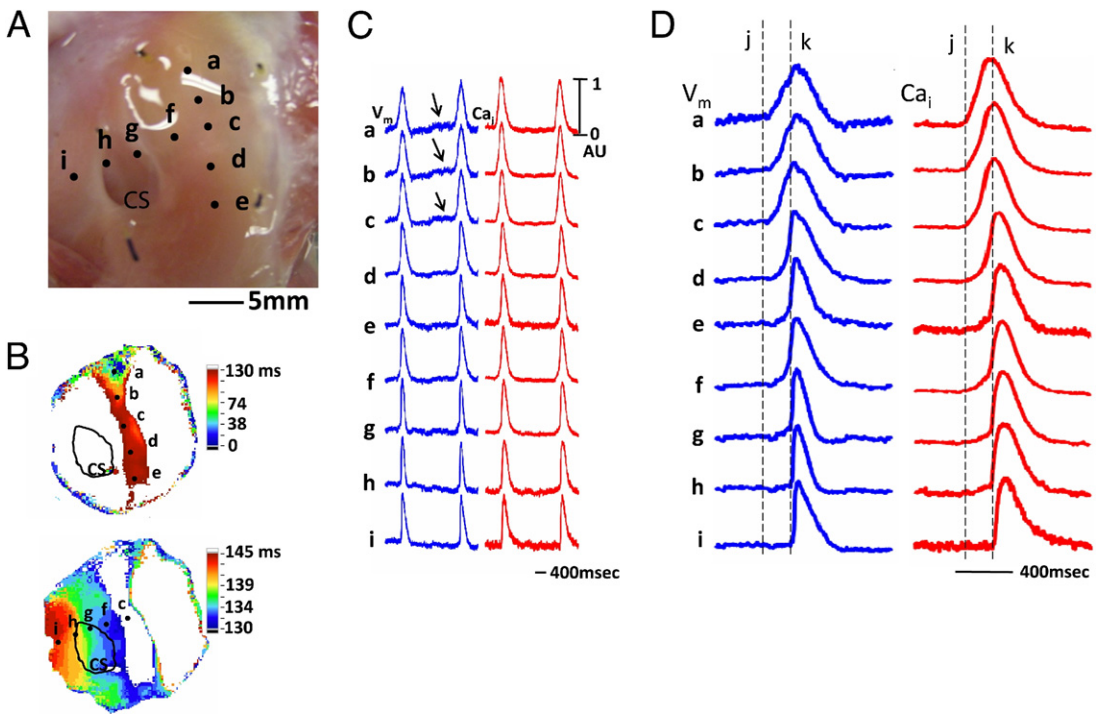

Figure 2 Optical Recording During Spontaneous AVJ Rhythm

(A) Filled circles represent optical recording sites. **a** indicates the earliest activation site. **(B)** Isochronal activation map during spontaneous AVJ rhythm shows slow conduction toward the area between CS and tricuspid valve. After a delay, the wavefront conducted rapidly away and excited the entire atrium. **(C)** Optical V_m **(blue)** and Ca_i **(red)** tracings during spontaneous AVJ rhythm. **Arrows** point to phase 4 diastolic depolarization near the AVN. **(D)** Same tracings shown in greater detail. The **vertical dashed line j** indicates the time of action potential onset at site **a**. The **vertical dashed line k** indicates the time of action potential onset at site **i**. Abbreviations as in Figure 1.

characteristics of their optical signals (9). Specifically, the AVN was identified as sites with slow phase 0 with a notch (arrow) that corresponded temporally with the His potential registered by an electrophysiological catheter in the His area (bottom tracing). The location of the AVN was confirmed microscopically (red arrow, Fig. 1C). The HCN4 staining was positive in the AVN and negative in the surrounding tissues (Fig. 1D).

Characterization of AVJ rhythm. Baseline AVJ rhythm had a rate of 37.5 ± 4.0 beats/min. Figure 2A shows the mapped region. Among them, sites a, b, and c corresponded to the anatomical location of the AVN. Figure 2B shows the isochronal activation map of a single beat during the typical AVJ rhythm, with the earliest activation in the leading pacemaker site as time 0. In the all cases at baseline, the AVJ rhythm began near AVN and slowly propagated toward SP region inferior to AVJ (Fig. 2B, top), and then rapidly propagates toward the other parts of the atrium (Fig. 2B, bottom). In this example, the former portion of the propagation took 130 ms and the latter portion only 15 ms (from 130 to 145 ms). There was an obvious conduction delay between AVN region and the rest of the RA preparation. Figure 2C shows the optical signals recorded at different sites shown in Figure 2B. There was diastolic depolarization (arrows) at the leading pacemaking site near AVN. These diastolic depolarizations occurred without preceding LDCAE on the Ca_i tracing. Panel 2D shows these optical signals in greater detail. The upstroke slope of optical V_m and Ca_i fluorescence was shallow in the AVN and the slow pathway (sites a through d). There was very slow propagation between sites c and f. The propagation from f to i was fast and was associated with a steep slope in the phase 0. The delay between phase 0 of site c and phase 0 of site f in all preparations averaged 102 ± 25.5 ms.

Effects of pharmacologic interventions. BETA-ADRENERGIC STIMULATION. Isoproterenol increased the rate of AVJ rhythm in a dose-dependent fashion from 0.01 to 3.0 μmol/l (Fig. 3A). In all preparations studied, the heart rate increased by a maximum of 167.2% (from 37.5 ± 4.0 beats/min to 100.2 ± 6.8 beats/min) during isoproterenol infusion. The slope of DD progressively decreased as the distance between the recording site and the leading pacemaker site progressively increased (Fig. 3B). We also noted that LDCAE appeared at the leading pacemaker sites in all 6 preparations during

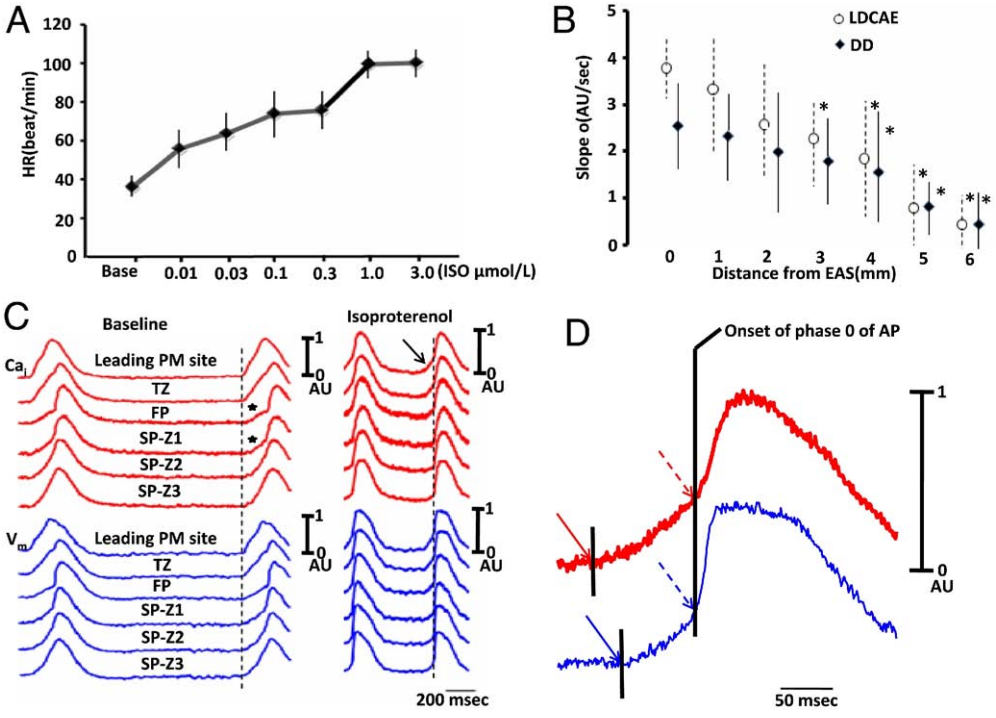

Figure 3 Effects of Isoproterenol

(A) Dose-response relationship between heart rate (HR) and isoproterenol (ISO). **(B)** The relationship between the slope and distance from the leading pacemaker (LP) site for late diastolic Ca elevation (LDCAE) and diastolic depolarization (DD). **Asterisks** indicate significant difference ($p \leq 0.05$) between the slopes at the EAS and at sites distant from EAS. **(C)** The Ca_i **(red)** and V_m **(blue)** tracings at baseline and during isoproterenol infusion. At baseline, the initial portions of the FP and SP-Z1 **(asterisks)** showed gradual rise of V_m, suggesting that these sites have recorded optical signals from anatomical layers that activated earlier. During isoproterenol infusion, LDCAE **(arrow)** occurred before phase 0 **(vertical dashed line)** of the leading pacemaker. **(D)** Magnified view of Ca_i and V_m tracings of AVN during isoproterenol infusion. The onset of LDCAE **(solid red arrow)** was noted before the onset of action potential **(solid blue arrow)**. The **red dashed arrow** indicates peak LDCAE and the **blue dashed arrow** indicates peak DD. The **vertical line segment** indicates the onset of the phase 0 of action potential. EAS = earliest activation site; PM = pacemaker; other abbreviations as in Figure 1.

isoproterenol infusion (Fig. 3C, arrow). LDCAE at the leading pacemaker site preceded the phase 0 action potential upstroke by 97.3 ± 35.2 ms and preceded the onset of late DD by 23.5 ± 3.5 ms (Fig. 3D). Similar to DD, the slope of LDCAE progressively decreased as the distance from pacing site increased (Fig. 3B). In this (Fig. 3C) and an additional 3 preparations, the same site served as the leading pacemaker both at baseline and during isoproterenol infusion. In 4 preparations, however, the leading pacemaker sites shifted during isoproterenol infusion. At the leading pacemaker sites, the slopes of LDCAE are 0 AU/s, 1.47 ± 0.16 AU/s, 2.04 ± 0.18 AU/s, 2.93 ± 0.18 AU/s, 3.38 ± 0.27 AU/s, and 4.00 ± 0.21 AU/s with 0, 0.01, 0.03, 0.1, 0.3, and 1.0 μmol/l of isoproterenol, respectively ($p < 0.001$). The slopes of DD are 0 AU/s, 0.55 ± 0.15 AU/s, 0.95 ± 0.16 AU/s, 1.40 ± 0.15 AU/s, 1.93 ± 0.10 AU/s, and 2.28 ± 0.10 AU/s with 0, 0.01 l, 0.03, 0.1, 0.3, and 1.0 μmol/l of isoproterenol, respectively ($p < 0.001$). Post hoc tests showed that there were significant differences among all groups, with p values ranging from 0.000 to 0.001 for LDCAE and from 0.000 to 0.0038 for DD.

Figure 4A summarizes the responses to isoproterenol of all preparations studied. Arrows in Figure 4A show the original leading pacemaker site (solid black dots) and the leading pacemaking sites during isoproterenol infusion (open black dots). The filled red dots indicate sites where there were no shifts. Figure 4B shows the isochronal activation maps and the corresponding Ca_i maps of preparation, labeled "3" in Figure 4A. The baseline activation originated in the AVN region (site a, blue color). The activation then shifted downward with 0.01 μmol/l isoproterenol (site b). Further increase of dose to 0.1 μmol/l resulted in a leftward shift to site c. Figure 4C shows that the sites of LDCAE (arrows) shifted along with the leading pacemaker site. In all 4 preparations with shifting leading pacemaker sites, the LCDAE always colocalized with the leading pacemaker site.

CAFFEINE. We gave caffeine as a 2-ml bolus (20 mmol/l) directly into the left circumflex artery in 2 preparations. Figure 5A shows the direction of impulse propagation (arrows) along the SP and FP. Figures 5B and 5C show Ca_i and V_m tracings along the SP and FP, respectively, during caffeine infusion. Arrows point to LDCAE at the leading pacemaker (LP) site. Figure 5D shows actual V_m and Ca_i recorded at baseline and during caffeine infusion at LP, FP, and SP. The slopes of LDCAE (3.25 ± 0.14 AU/s) and DD (2.41 ± 0.05 AU/s) during caffeine infusion are significantly steeper than LDCAE and DD at baseline (0 AU/s, $p = 0.020$; and 0.27 ± 0.16 AU/s, $p = 0.022$, respectively). LDCAE (arrows) appeared in the LP site, and the mean AVJ rate increased by 108% (from 37.5 ± 4.0 beats/min to 78.3 ± 3.2 beats/min). In these 2 prepa-

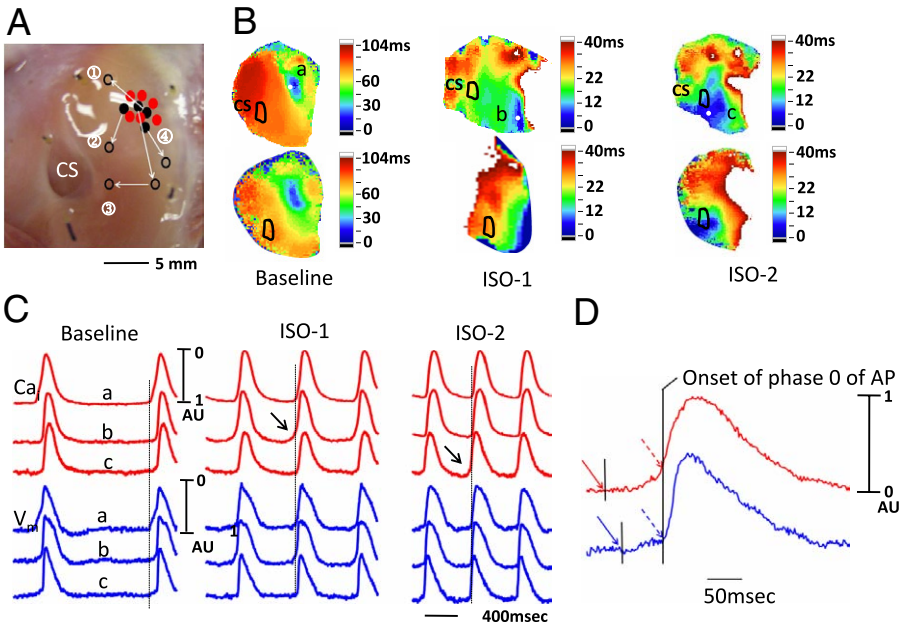

Figure 4 **Shift of Leading Pacemaker Sites During Isoproterenol Infusion**

(A) Directions of the shifts of all preparations are shown. **(B)** Isochronal activation maps showing shift of leading pacemaker site in heart #3 during isoproterenol infusion. The **upper and lower parts** are V_m and Ca_i isochronal activation maps, respectively. This case shows pacemaker shifts from baseline **a** site to **b** and then to **c** site during isoproterenol infusion. **(C)** Optical V_m and Ca_i recording in same case. **(D)** Magnified view of Ca_i and V_m tracings of early activation site **(C)** at ISO-2. A robust late diastolic Ca elevation (LDCAE) **(arrow)** always colocalized with leading pacemaker site. **Vertical broken lines** indicate the onset of action potential in the leading pacemaker site. The onset of LDCAE **(solid red arrow)** was noted before the onset of action potential **(solid blue arrow)**. The **red dashed arrow** indicates peak LDCAE and the **blue dashed arrow** indicates peak diastolic depolarization. ISO-1 = isoproterenol 0.01 μmol/l; ISO-2 = isoproterenol 0.1 μmol/l; other abbreviations as in Figure 1.

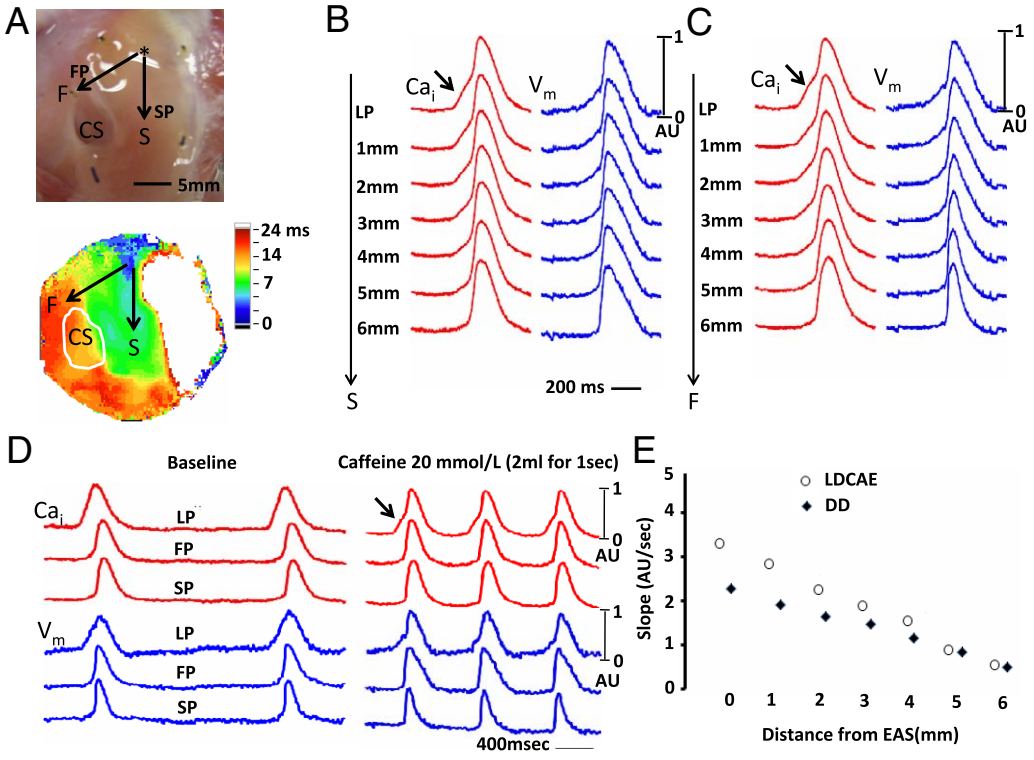

Figure 5 Spatial Changes of Ca_i and V_m Around the Leading Pacemaker Site After Caffeine Injection

(A) Upper panel shows the area mapped. An **asterisk** marks the site of the LP. The **arrow** along SP is labeled **S**, whereas the **arrow** along the FP is labeled **F**. **Lower panel** shows isochronal activation map after caffeine injection. **(B)** The changes of V_m **(blue)** and Ca_i **(red)** tracings along SP direction. **(C)** The changes of V_m **(blue)** and Ca_i **(red)** tracings along FP direction. **(D)** The Ca_i **(red)** and V_m **(blue)** tracings at baseline and after caffeine injection. The **arrow** indicates late diastolic Ca elevation (LDCAE). **(E)** The relationship between the slope and distance from the leading pacemaker (LP) site for LDCAE and diastolic depolarization (DD). CS = coronary sinus; EAS = earliest activation site; other abbreviations as in Figure 1.

rations, the LP sites did not shift locations during caffeine infusion. Similar to that seen during isoproterenol infusion, the sites with maximum slopes of LDCAE and DD always colocalized with the LP sites. The slopes decreased progressively as the recording sites moved away from the LP site (Fig. 5E).

RYANODINE. Figure 6 shows the effects of ryanodine in 1 preparation. Ryanodine 3 μmol/l markedly slowed the rate of spontaneous AVJ rhythm by 83.2%, from 37.5 ± 4.0 to 6.3 ± 6.2 beats/min (Fig. 6A). Isoproterenol infusion after ryanodine (n = 2) increased the heart rate only to 16.4 ± 6.3 beats/min, which was 56.2% less than the baseline rate before ryanodine (Fig. 6A). Figure 6B shows that ryanodine reduced the AVJ rate in a preparation receiving isoproterenol infusion. Isoproterenol did not induce LDCAE in the presence of ryanodine, and the heart rate increase was not associated with LDCAE (Fig. 6C).

ZD 7288. The I_f blocker ZD 7288 (3 μmol/l) decreased basal AVJ rate by 35% (n = 2). The ZD 7288 did not prevent 1.0 μmol/l of isoproterenol from increasing AVJ rate by 158% (p = 0.011, compared with basal rate), accompanied by the appearance of LDCAE with LP shifted to the upper site in the AVN. There was apparent LDCAE at the LP site (Fig. 7B).

Discussion

The present study shows that isoproterenol and caffeine-induced AVJ rhythm acceleration was accompanied by increased LDCAE. The isoproterenol effects were suppressed by ryanodine, but not by ZD 7288. There was colocalization of the maximum LDCAE with the LP sites in the AVJ. These findings suggest that spontaneous SR Ca release plays an important role in the mechanisms of AVJ rate acceleration during isoproterenol or caffeine infusion. A functioning Ca clock in the AVJ is important to the generation of heart rhythm when SAN is impaired or not present.

Mechanisms of AVJ rhythm. Whether or not the studies of SAN can be directly applied to the mechanisms of AVJ rhythm acceleration during isoproterenol infusion is unclear. Because the AVN and posterior extension express HCN4 (channel responsible for I_f), it is plausible to hypothesize that I_f is responsible for the AVJ automaticity (11). The present study shows that in addition to I_f and the membrane voltage clock, the Ca clock is also important in

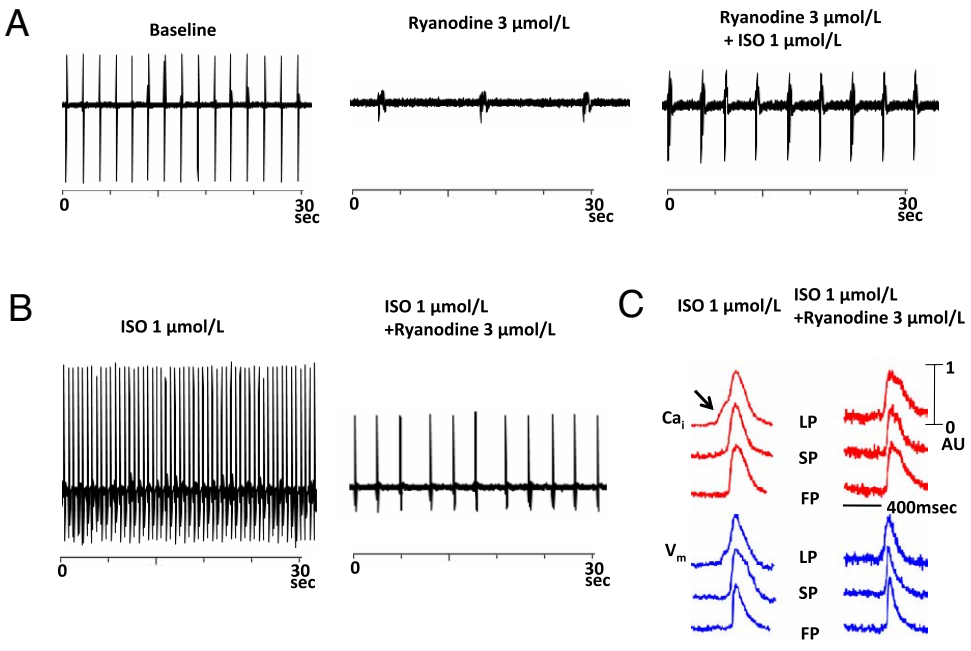

Figure 6 The Effect of Ryanodine on Automaticity of Intact Canine AVN

(A) Ryanodine 3 μmol/l markedly slowed the rate of AVJ rhythm by 83.2% **(middle)**. Isoproterenol infusion after ryanodine increased the heart rate only to 16.4 ± 6.3 beats/min **(right)**. **B** shows that the effects of isoproterenol on heart rate were significantly suppressed by ryanodine. **(C)** Effect of ryanodine on the isoproterenol-induced late diastolic Ca elevation (LDCAE). Ryanodine completely abolished the LDCAE **(arrow)**. ISO = isoproterenol; LP = leading pacemaker; other abbreviations as in Figure 1.

AVJ automaticity. Unlike SAN, the anatomic location of the AVJ pacemaker in rabbit heart is stable during autonomic modulation (12). Consistent with that finding, the LP sites in a majority of preparations in our study do not move during isoproterenol infusion. However, in 4 preparations, the LP sites do move with isoproterenol. More importantly, simultaneous Ca_i and V_m mapping showed that LDCAE preceded the onset of late DD and that the LP site always colocalized with the maximum slope of the LDCAE. Ryanodine was more effective than ZD 7288 in

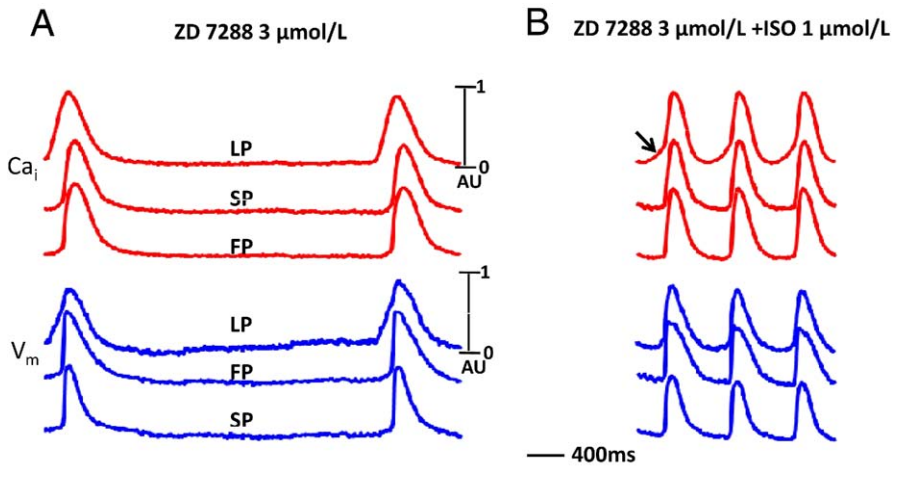

Figure 7 The Effect of ZD 7288 on Intact Canine AVN

(A) The Ca_i and V_m tracing during a 3-μmol/l ZD 7288 infusion. **(B)** Isoproterenol 1 μmol/l produced late diastolic Ca elevation **(arrow)** at the leading pacemaker site (LP) in the presence of ZD 7288. ISO = isoproterenol; other abbreviations as in Figure 1.

preventing heart rate acceleration induced by isoproterenol. Ridley et al. (8) isolated myocytes from the AVN of rabbit hearts and performed optical mapping of the Ca_i transients in those myocytes. They found that there are spontaneous Ca_i transients in the AVN cells. These transients ramped up the amplitude before the onset of the upstroke of the Ca_i. The morphology of the Ca_i ramp in that study was the same as the LDCAE at the LP sites in the present study. The authors also reported that ryanodine inhibited the spontaneous Ca_i transients and reduced the rates of spontaneous activation. Our study extended their observations to the intact AVJ. The availability of simultaneous V_m signals confirmed that these Ca_i ramps described by Ridley et al. (8) in fact occurred before the onset of the phase 0 of the action potential. Taken together, these data indicate that SR Ca clock plays an important role in AVJ automaticity.

Study limitations. Optical signals collected from the canine 3-dimensional tissues represent a weighted average of the transmembrane action potentials throughout the entire canine atrial wall (13). It is possible that the little foot in front of the optically recorded action potential or Ca_i transients is not DD or LDCAE, but rather a strongly filtered optical recording from the deeper structures. However, as shown in Figure 4C, the site of Ca_i elevation moves from one site to another during isoproterenol infusion, and it always colocalizes with the earliest site of activation on the isochronal map. Similarly, the DD in LP site occurs during isoproterenol infusion but not at baseline (Fig. 3C). These findings rule out a fixed deeper structure as a source of these isoproterenol-induced deflections.

Because of the complex origin of the impulse near the AVJ, it is possible that activation propagated from the SAN might contaminate the signals of the AVJ (14,15). Therefore, we trimmed away the sinus node in the present study, allowing the impulse originated from AVJ itself to propagate toward the surrounding atrial myocardium. The late DD and the first action potential upstroke observed in the AVJ region therefore represent signals initiated in the AVJ. The second upstroke in the optical signal represents the signals of a different layer (the nonpacemaking atrial myocardium) that was excited by the AVJ pacemaker. We propose that late DD and LDCAE are not affected by the activations of nonpacemaking cells in this study.

Acknowledgments

The authors thank Jian Tan, Yanhua Zhang, and Lei Lin for their assistance.

Reprint requests and correspondence: Dr. Peng-Sheng Chen, Krannert Institute of Cardiology, 1801 North Capitol Avenue, E475, Indianapolis, Indiana 46202. E-mail: chenpp@iupui.edu.

REFERENCES

1. Lakatta EG, Maltsev VA, Vinogradova TM. A coupled SYSTEM of intracellular Ca2+ clocks and surface membrane voltage clocks controls the timekeeping mechanism of the heart's pacemaker. Circ Res 2010;106:659–73.
2. Maltsev VA, Lakatta EG. Synergism of coupled subsarcolemmal Ca2+ clocks and sarcolemmal voltage clocks confers robust and flexible pacemaker function in a novel pacemaker cell model. Am J Physiol Heart Circ Physiol 2009;296:H594–615.
3. Joung B, Tang L, Maruyama M, et al. Intracellular calcium dynamics and acceleration of sinus rhythm by beta-adrenergic stimulation. Circulation 2009;119:788–96.
4. Racker DK, Kadish AH. Proximal atrioventricular bundle, atrioventricular node, and distal atrioventricular bundle are distinct anatomic structures with unique histological characteristics and innervation. Circulation 2000;101:1049–59.
5. Racker DK. Sinoventricular transmission in 10 mM K+ by canine atrioventricular nodal inputs. Superior atrionodal bundle and proximal atrioventricular bundle. Circulation 1991;83:1738–53.
6. Convery MK, Hancox JC. Na+-Ca2+ exchange current from rabbit isolated atrioventricular nodal and ventricular myocytes compared using action potential and ramp waveforms. Acta Physiol Scand. 2000;168:393–401.
7. Hancox JC, Levi AJ, Brooksby P. Intracellular calcium transients recorded with Fura-2 in spontaneously active myocytes isolated from the atrioventricular node of the rabbit heart. Proc Biol Sci 1994;255:99–105.
8. Ridley JM, Cheng H, Harrison OJ, et al. Spontaneous frequency of rabbit atrioventricular node myocytes depends on SR function. Cell Calcium 2008;44:580–591.
9. Wu J, Olgin J, Miller JM, Zipes DP. Mechanisms underlying the reentrant circuit of atrioventricular nodal reentrant tachycardia in isolated canine atrioventricular nodal preparation using optical mapping. Circ Res 2001;88:1189–95.
10. Inoue S, Becker AE. Posterior extensions of the human compact atrioventricular node: a neglected anatomic feature of potential clinical significance. Circulation 1998;97:188–93.
11. Hucker WJ, Nikolski VP, Efimov IR. Optical mapping of the atrioventricular junction. J Electrocardiol 2005;38:121–5.
12. Hucker WJ, Nikolski VP, Efimov IR. Autonomic control and innervation of the atrioventricular junctional pacemaker. Heart Rhythm 2007;4:1326–35.
13. Fedorov VV, Schuessler RB, Hemphill M, et al. Structural and functional evidence for discrete exit pathways that connect the canine sinoatrial node and atria. Circ Res 2009;104:915–23.
14. Efimov IR, Mazgalev TN. High-resolution, three-dimensional fluorescent imaging reveals multilayer conduction pattern in the atrioventricular node. Circulation 1998;98:54–57.
15. Efimov IR, Fedorov VV, Joung B, Lin SF. Mapping cardiac pacemaker circuits: methodological puzzles of the sinoatrial node optical mapping. Circ Res 2010;106:255–71.

Key Words: automaticity ■ sympathetic stimulation ■ optical mapping ■ electrophysiology ■ arrhythmia.